

論文 / 著書情報  
Article / Book Information

Title	Visualizing positive and negative charges of triboelectricity generated on polyimide film
Authors	Dai Taguchi, Takaaki Manaka, Mitsumasa Iwamoto
Citation	IEICE Transactions on Electronics, Vol. E104-C, No. 6, pp. 170-175
Pub. date	2021, 6
Copyright	Copyright(C)2021 IEICE

# Visualizing Positive and Negative Charges of Triboelectricity Generated on Polyimide Film

Dai TAGUCHI<sup>†</sup>, Takaaki MANAKA<sup>†</sup>, *Members*, and Mitsumasa IWAMOTO<sup>†a)</sup>, *Fellow*

**SUMMARY** Triboelectric generator is attracting much attention as a power source of electronics application. Electromotive force induced by rubbing is a key for triboelectric generator. From dielectric physics point of view, there are two microscopic origins for electromotive force, i.e., electronic charge displacement and dipolar rotation. A new way for evaluating these two origins is an urgent task. We have been developing an optical second-harmonic generation (SHG) technique as a tool for probing charge displacement and dipolar alignment, selectively, by utilizing wavelength dependent response of SHG to the two origins. In this paper, an experimental way that identifies polarity of electronic charge displacement, i.e., positive charge and negative charge, is proposed. Results showed that the use of local oscillator makes it possible to identify the polarity of charges by means of SHG. As an example, positive and negative charge distribution created by rubbing polyimide surface is illustrated.

**key words:** electric-field-induced optical second-harmonic generation, orientational order parameter, dipolar rotation, charge displacement, Maxwell's displacement current

## 1. Introduction

Triboelectric generator has been known for long time as an electrical generator [1], [2]. By rubbing an insulator by metal, semiconductor, etc., charge displacement is induced and mechanical power transfers to electrical power. Recently, new synthesis of insulating polymers and new processing technique development allows enhancement of surface power density to 30 mW/cm<sup>2</sup> [3]. Micro- and nano-structured surface of materials are utilized to enhance power density. Accordingly, research and development (R&D) of triboelectric generator is freshly being activated. For example, the triboelectric generator for switching electronic paper display [4], switching memory devices [5], power supply with non-connecting power line [6], and so on, have been reported.

Idea of triboelectric series has been utilized for the choice of appropriate combination of materials for triboelectric generation. However, emergence of micro- and nano-structure surface for high power density generator tells us that this situation is no longer sufficient to establish a new scientific basis. That is, not only material property but also microscopic structure of materials is a key for making clear triboelectric generation process.

A high-tech analytical tool such as, energy-filtered

transmission electron microscopy (EFTEM) [7], is available from physicochemical aspects. Electronic energetics have been investigated by using ultraviolet photoelectron spectroscopy (UPS) [8] and electrostatic potentials and so on in micro and nano scales have been visualized by using Kelvin probe force microscopy (KPFM) [9]. In terms of dielectric physics, there are two microscopic origins for electric power generation [10]. One is charge displacement and the other one is dipole rotation. Accordingly, an experimental technique that identifies the two microscopic origins is of importance to investigate carrier processes in triboelectric generation. The authors have been developing optical second-harmonic generation (SHG) measurement as a method that allows one to identify charge displacement and dipolar alignment. SHG measurement can probe, selectively, charge displacement at laser wavelength  $\lambda_1$  and dipolar alignment at  $\lambda_2$  ( $\neq \lambda_1$ ) [11], [12]. But this situation is no longer sufficient. EFTEM and KPFM investigations showed that positive and negative charges are microscopically distributed after rubbing polymers, and we need to identify polarity of charges created on polymer surface.

The purpose of this paper is to show that the SHG measurement can identify the polarity of charges and visualize the distribution of positive and negative charges. The SHG measurement system introducing local oscillator technique is shown to be effective for this purpose. As an example, positive and negative charge distributions remained on polyimide tape are visualized by using the SHG measurement using the local oscillator (quartz) [13].

## 2. Experiment

### 2.1 Sample

Figure 1 (a) shows a typical chemical structure of polyimide adhesive tape used in experiment. The polyimide layer thickness is 25  $\mu\text{m}$  and adhesive layer is provided to fix the polyimide on a Ni-foil. The rubbing of polyimide surface is carried out by using cotton and polytetrafluoroethylene (PTFE) film, in the direction along the incident plane of laser beam (Fig. 2). The impressed force of the rubbing is about 5 N in normal direction to polyimide surface. The rubbing was in one-directional way, i.e., the direction from left to right as indicated in Fig. 2. Preliminary experiment of surface potential measurement was carried out to get information on the polarity of surface potential created after rubbing. After rubbing the polyimide surface by cotton,

Manuscript received July 22, 2020.

Manuscript revised October 7, 2020.

Manuscript publicized October 23, 2020.

<sup>†</sup>The authors are with School of Engineering, Tokyo Institute of Technology, Tokyo, 152–8552 Japan.

a) E-mail: iwamoto@pe.titech.ac.jp

DOI: 10.1587/transele.2020OMP0001

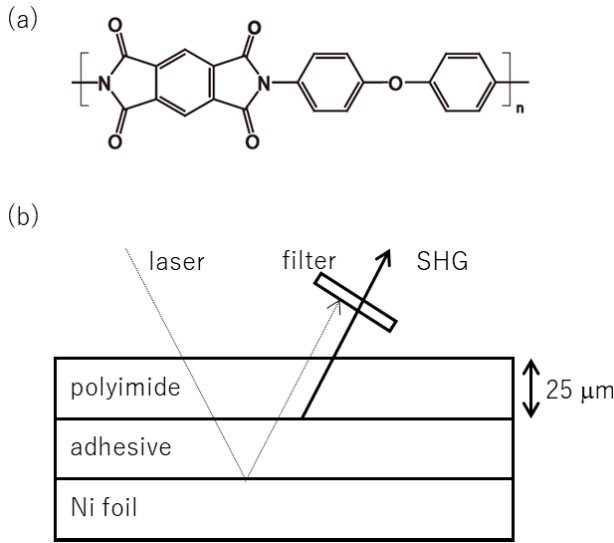


**Fig. 1** (a) A typical chemical structure of polyimide used in experiment. (b) A polyimide tape fixed on Ni foil used for SHG experiment.

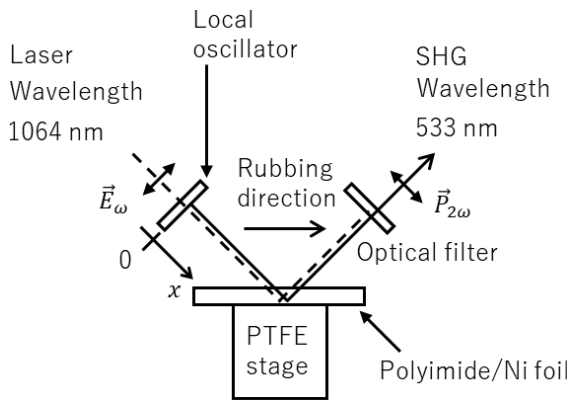


**Fig. 2** SHG measurement arrangement where local oscillator is installed for to distinguish polarity of charge induced in a course of rubbing.

polyimide surface potential is established negatively  $-1500$  V. The rubbing by PTFE film induces positive potential  $+500$  V across the polyimide film. The surface potential value was measured in reference to Ni-foil. Note that the polarity of surface potential well agrees to that expected from the general tendency of charging of materials, which is known as triboelectric series (an example of triboelectric series is described in Ref. [3]). According to the triboelectric series, among materials used in the SHG measurement, cotton is positioned on the most positive side, and then polyimide. Meanwhile, PTFE is positioned on the most negative side. Triboelectric series suggests that positive charges tend to remain on a material positioned on the positive side, if this material is rubbed with another material positioned on the negative side. Accordingly, by rubbing polyimide with cotton, triboelectric series suggests that cotton and polyimide, respectively, will be charged positively and negatively. In a similar way, by rubbing polyimide with PTFE, polyimide is expected to be positively charged after rubbing.

The Ni-foil was electrically grounded and used as a reference electrode for intentionally charging and discharging polyimide surface. The charging and discharging of polyimide surface were carried out by using conductive brush where external high voltage is applied in reference to the Ni-foil grounded. The voltage  $V = 0$  V is applied for discharging polyimide surface.  $V = +2$  kV and  $-2$  kV are applied for charging. The surface potential of polyimide surface was measured by using Kelvin probe, and was used for confirming the polarity of surface potential after applying conductive brush.

## 2.2 SHG Measurement

SHG is nonlinear optical process where electric field  $\vec{E}_\omega$  of probe laser beam vibrating at angular frequency  $\omega$  induces nonlinear polarization at double frequency  $2\omega$ , in a course of electromagnetic coupling between electromagnetic wave and electrons in materials. As a result of the electromagnetic coupling, optical second nonlinear polarization  $\vec{P}_{2\omega}$  is induced in materials as

$$\vec{P}_{2\omega} = \epsilon_0 \vec{\chi}^{(2)} : \vec{E}_\omega \vec{E}_\omega + \epsilon_0 \vec{\chi}^{(3)} : \vec{E}_0 \vec{E}_\omega \vec{E}_\omega + \vec{P}_h, \quad (1)$$

where the first term is SHG, the second term is electric-field-induced SHG (EFISHG), and the last term  $\vec{P}_h$  is higher order SHG processes.  $\epsilon_0$  is dielectric permittivity of vacuum.  $\vec{\chi}^{(2)}$  is related to symmetry of materials, and is available to selectively probe dipolar alignment [14], [15].  $\vec{\chi}^{(3)}$  expresses the nonlinear property of materials where electrostatic field  $\vec{E}_0$  deviates electrons cloud in molecules, allowing us to probe electronic charge displacement by means of EFISHG measurement. It is worth noting that  $\vec{\chi}^{(2)}$  and  $\vec{\chi}^{(3)}$  exhibit resonance enhancement at different laser wavelength. In triboelectric generation process, both charge displacement and dipolar rotation contribute to electrical work consumed in an external circuit. By choosing laser wavelength  $\lambda = \lambda_1$  at which  $\vec{\chi}^{(3)}$  is dominant and  $\vec{\chi}^{(2)}$  is minor, we can selectively visualize charge displacement [12]. By selecting laser wavelength  $\lambda = \lambda_2$  at which  $\vec{\chi}^{(2)}$  governs second-harmonic polarization and  $\vec{\chi}^{(3)}$  is absent, we can probe alignment of dipoles. In the experiment described here, we set the laser wavelength  $\lambda_1 = 1064$  nm (SHG wavelength 532 nm), to selectively probe charge displacement. At  $\lambda = \lambda_1$ , Eq. (1) is

$$\vec{P}_{2\omega} = \epsilon_0 \vec{\chi}^{(3)} : \vec{E}_0 \vec{E}_\omega \vec{E}_\omega \quad (2)$$

This polarization  $\vec{P}_{2\omega}$  with nonzero  $\vec{\chi}^{(3)}$  is available to probe electrostatic field  $\vec{E}_0$  formed in materials. However, it is not possible to determine polarity of electrostatic field by measuring EFISHG light intensity  $I_{2\omega}$  from the polarization  $\vec{P}_{2\omega}$  in Eq. (2). That is, the light intensity is proportional to the square of polarization:

$$I_{2\omega} \propto |\vec{P}_{2\omega}|^2 = |\vec{E}_0|^2 \quad (3)$$

Equation (3) shows that  $\vec{E}_0$  and  $-\vec{E}_0$  gives the same SHG intensity  $I_{2\omega} = |\vec{E}_0|^2 = |-\vec{E}_0|^2$ . We cannot determine the polarity of  $\vec{E}_0$ . Accordingly, local oscillator is freshly necessary to determine both the intensity and phase of second-harmonic polarization  $\vec{P}_{2\omega}$  [16]. The local oscillator produces second harmonic polarization  $\vec{P}_L = P_L e^{j\theta}$  with known phase  $\theta$ , and  $\vec{P}_L$  interferes with EFISHG as

$$\vec{P}_{2\omega} = \epsilon_0 \chi^{(3)} : \vec{E}_0 \vec{E}_\omega \vec{E}_\omega + \vec{P}_L, \quad (4)$$

The first term on right-hand side is the polarization from sample, and interferes with  $\vec{P}_L$  from the local oscillator. Note that experimentally, we control phase  $\theta$  by changing optical path length between local oscillator and sample by utilizing difference of refractive index of air at laser wavelength  $\lambda$  and at SHG wavelength  $\lambda/2$  [16]. Assuming that  $\chi^{(3)} = \chi_{zzzz}^{(3)}$  is dominant, the component of  $\vec{P}_{2\omega}$  (Eq. (4)) in  $z$ -direction (unit vector  $\hat{z}$  along the film thickness direction) is described as

$$\vec{P}_{2\omega} \cdot \hat{z} = A(E_0 + B e^{j\theta}) \quad (5)$$

with  $A = \epsilon_0 \chi^{(3)} E_\omega E_\omega$  and  $B = \frac{P_L}{\epsilon_0 \chi^{(3)} E_\omega E_\omega}$

By setting  $B > E_0$ , SHG intensity  $I_{2\omega} \propto |P_{2\omega}|^2$  is periodic function of  $\theta$ . By setting optical arrangement so that  $\theta = 0$ , positive electric field ( $E_0 > 0$ ) constructively interferes with SHG from local oscillator, increasing total SHG intensity. Negative electric field ( $E_0 < 0$ ) decreases SHG intensity due to destructive interference of EFISHG with  $\vec{P}_L$  from the local oscillator. In this way, we can distinguish positive and negative charge displacement originating positive and negative electrostatic field  $E_0$ .

In experiment, we arranged local oscillator in SHG measurement system as displayed in Fig. 2. A variety of SHG setups shown in Fig. A-1 in Appendix are trialed. Among them, stable SHG interference is found to be achieved by using the system illustrated in Fig. 2. As a probe laser beam, Q-switched Neodymium doped yttrium-aluminum-garnet (Nd:YAG) laser with wavelength  $\lambda_1 = 1064$  nm (repetition rate 10 Hz, pulse duration 4 ns, average power 10 mW, laser beam diameter 3 mm) is installed. SHG is available to probe charge displacement and dipole separately by selecting appropriate laser wavelength. At the wavelength  $\lambda_1 = 1064$  nm, charge displacement in polyimide is selectively probed [12]. Local oscillator is a quartz plate with a thickness of 1 mm (Y-cut quartz with a mark on  $x$ -crystal axis direction, Kogakugiken Co.). Accordingly,  $p$ -polarized laser beam was incident on local oscillator and on polyimide, and  $p$ -polarized SHG is selected by using a linear polarizer.

The SHG measurement was carried out in 3 steps as described in the following. In Step 1, correct position of local oscillator is determined where phase difference  $\theta$  is zero or  $\pi$ . Polyimide surface is positively and negatively charged by applying conductive brush connected to high voltage source (+2 kV and -2 kV). Positive charges remained on polyimide surface after corona-discharge by +2 kV. According

to Gauss law in electromagnetism, positive charge on polyimide surface forms electrostatic field in the direction originating from positive charge on polyimide surface toward negative charge induced on Ni-foil surface ( $E_0 > 0$ ). Negative charges remain on polyimide surface after charging at -2 kV. Electrostatic field in the polyimide is pointing in the direction from Ni surface toward polyimide surface ( $E_0 < 0$ ). With the known polarity of charges on polyimide surface, local oscillator was shifted toward the polyimide sample to sweep phase difference  $\theta$  between SHG  $\vec{P}_L$  from local oscillator and SHG  $\epsilon_0 \chi^{(3)} : \vec{E}_0 \vec{E}_\omega \vec{E}_\omega$  from polyimide (see Eq. (5)). The SHG light was detected by using photomultiplier tube (PMT) in the experiment.

In step 2, the local oscillator is set at the position satisfying  $\theta = 0$  or  $\theta = \pi$ . In the following, the case of condition  $\theta = \pi$  ( $e^{j\theta} = -1$ ) is described. Equation (5) shows that negative electric field ( $E_0 < 0$ ) in polyimide results in constructive interfere with  $\vec{P}_L$ , resulting in increase of SHG intensity. Meanwhile, positive electric field cause decrease of SHG intensity. The same experimental procedure applies for the case of  $\theta = 0$  with opposite quality.

In Step 3, after rubbing polyimide film, positive and negative charges are visualized by imaging SHG on charge-coupled-device (CCD) camera (image A). The reference image (image B) with zero surface potential was recorded and subtracted numerically from the SHG image A, i.e., “image C” = “image A” – “image B” for every pixel of CCD camera. The positive and negative values of image C is an image of negative and positive electrostatic field in polyimide layer. The rubbing is carried out at 5 N applied to normal to surface of polyimide tape and repeated for 10 times in the direction indicated in Fig. 2. Note that after repeating rubbing in this condition, surface potential formed across the polyimide tape saturates.

### 3. Results and Discussion

Figure 3 shows SHG intensity recorded as a function of position of local oscillator (Sect. 2.2: Step 1). Figure 3 (a) is SHG from a polyimide after positively charging the surface of polyimide. Along with the shift of local oscillator position, SHG intensity increase from  $x = 0$  and arrive at maximum at  $x = 20$  mm. After that, the SHG intensity decreases to minimum at  $x = 80$  mm. Afterwards SHG intensity increases again. The result shows that SHG from local oscillator and SHG from polyimide interfere efficiently, causing periodic change of SHG intensity as expected from Eq. (5). Figure 3 (b) shows SHG intensity after negatively charging polyimide surface. The changing behavior of SHG intensity is similar to Fig. 3 (a), but the polarity is opposite. From  $x = 0$  to 20 mm, SHG intensity decreases, then increases to 80 mm. The result is consistent with Eq. (5) where polarity of  $E_0$  is opposite for positive electric field ( $E_0 > 0$ ) and negative electric field ( $E_0 < 0$ ). These results show that local oscillator technique is available to distinguish between positive and negative charges by using SHG measurement.



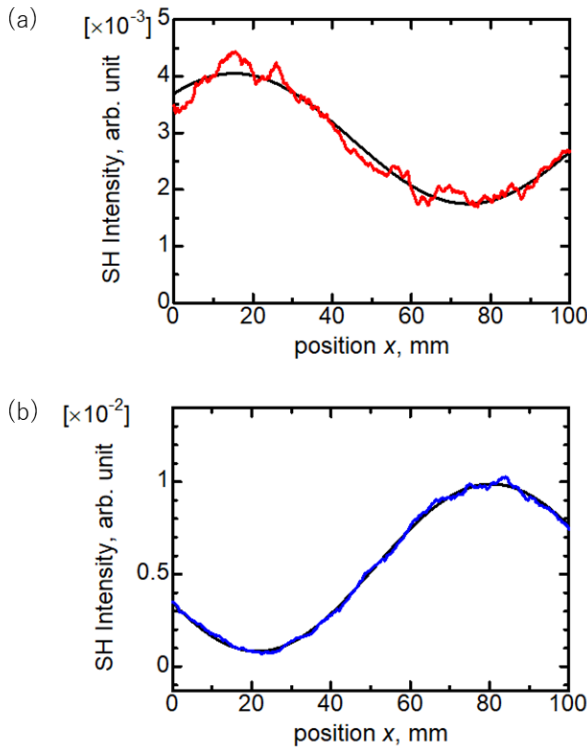


**Fig. 3** Interference between SHG from local oscillator (quartz) and EFISHG from polyimide. The interfered SHG intensity is plotted as a function of position  $x$  of the local oscillator. EFISHG is from (a) positively and (b) negatively charged polyimide film in reference to grounded Ni foil.

Figure 4 is examples of SHG image recorded with the local oscillator positioned at  $x = 80$  mm. By setting at this position, the phase difference condition is  $\theta = \pi$ . SHG intensity increases in an area where negative charge is on polyimide. By contrast, SHG intensity decreases in the region where positive charges remained on polyimide. In these figures, positive charges are printed in black and negative charges are white, and labeled by red and green color, respectively. It is noteworthy that the image of Fig. 4 is the difference between SHG image after rubbing and the reference image at zero surface potential. The SHG pattern originating from local oscillator dominates the raw SHG images and the difference SHG image clearly shows SHG change due to creation of positive and negative charges remained on a polyimide tape. Note that the SHG was detected by using PMT to record interference profile (Fig. 3) while CCD camera was installed to image charge distribution (Fig. 4). As a result, SHG intensity in Fig. 4 is in proportion to the vertical axis of interference measurement in Fig. 3.

Figure 4(a) shows that negative charges are created on polyimide surface after rubbing by cotton. The negative charges are distributed on whole area of the rubbed surface. Note that the laser spot is 3 mm diameter as indicated by the circle in Fig. 4, and governs the area where charges are imaged on a CCD camera. The result is consistent with the estimation from surface potential measurement that very large negative potential  $-1500$  V is established by

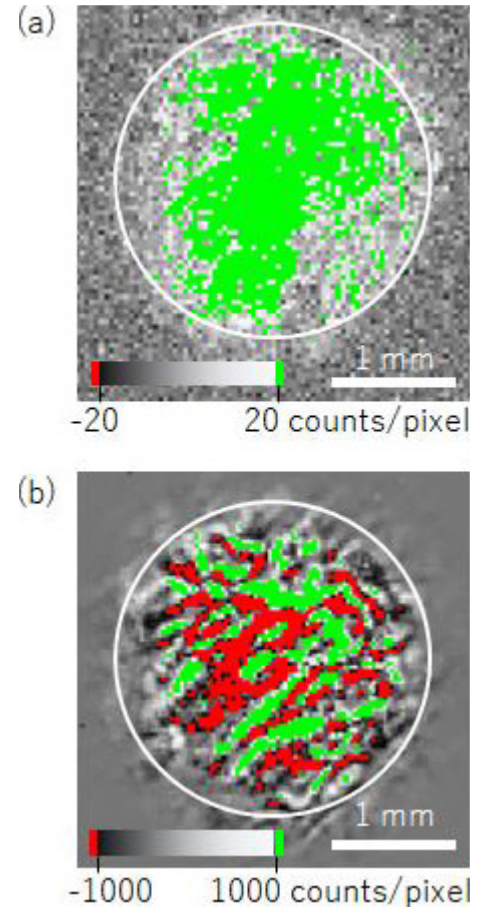


**Fig. 4** SHG image of polyimide tape surface after rubbing with (a) cotton and (b) PTFE. The change of SHG intensity is displayed in reference to the image taken in prior to the rubbing. The local oscillator is positioned at  $x = 80$  mm. SHG intensity increases (decreases) reflecting negative (positive) charges on polyimide surface created by the rubbing.

negative charges. On the other hand, after rubbing by using PTFE film, there are random domains of positive and negative charges separately on polyimide surface. The size of domain is, for example,  $810 \mu\text{m} \times 120 \mu\text{m}$ . As the Kelvin probe with 1 mm diameter was used to measure surface potential  $+500$  V, the positive and negative charges cancel their electrostatic potentials in average, resulting in smaller surface potential  $+500$  V.

It is noteworthy that generation of positive and negative charges after triboelectric generation process is known in milli-meter scale [7] and nano-meter scale [9]. In these reports, material transfer, chemical bond-breaking, etc., during a course of rubbing, were argued as a mechanism for creating both positive and negative charges, from physico-chemical aspects. The appearance of positive and negative charge after rubbing polyimide tape with PTFE may be similar phenomena, but we do not have a concrete idea on the mechanism at present.

#### 4. Conclusions

SHG measurement is an optical way that directly visualizes

triboelectricity. We have showed that the SHG measurement is available to identify two microscopic origins of triboelectric generation, i.e., charge displacement and dipolar alignment, and is helpful to visualize these microscopic origins separately at different probe laser wavelength. In this paper, we showed that the extra use of local oscillator (quartz plate) in SHG measurement further allows us to identify polarity of charges, i.e., positive and negative charges, in charge displacement origin. The results confirmed that this idea is effective in experiment.

### Acknowledgements

A part of this work is supported by Scientific research B, 17H03230. DT thanks TAENAKA PILE FABRICS Co., Ltd., for providing a rubbing cotton.

### References

- [1] M. Faraday, *Experimental Researches in Electricity*, Richard and John Edward Taylor, London, 1844.
- [2] J.C. Maxwell, *A Treatise on Electricity & Magnetism*, 3rd Edition, Dover, New York, 1954.
- [3] Z.L. Wang, "Triboelectric nanogenerators as new energy technology for self-powered systems as active mechanical and chemical sensors," *ACS Nano*, vol.7, pp.9533–9557, 2013.
- [4] M.E. Karagozler, I. Poupyrev, G.K. Fedder, and Y. Suzuki, "Paper generators: Harvesting energy from touching, rubbing, and sliding," *UIST '13 Proc. 26th annual ACM symposium on user interface software and technology*, Scotland, United Kingdom, pp.23–30, Oct. 8–11, 2013. DOI: 10.1145/2501988.2502054
- [5] A. Choudhary, T. Joshi, and A.M. Biradar, "Triboelectric activation of ferroelectric liquid crystal memory devices," *Appl. Phys. Lett.*, vol.97, p.124108, 2010.
- [6] O. Kawakami, "Functional Unit and Image Forming Apparatus," JP Patent A, 2007-286175, 2007. (in Japanese)
- [7] T.A.L. Burgo, T.R.D. Ducati, K.R. Francisco, K.J. Clinckspoor, F. Galembeck, and S.E. Galembeck, "Triboelectricity: Macroscopic charge patterns formed by self-arraying ions on polymer surfaces," *Langmuir*, vol.28, no.19, pp.7407–7416, 2012.
- [8] Y. Yamaguchi, K. Shimizu, A. Matsuzaki, D. Sano, T. Sato, Y. Tanaka, and H. Ishii, "Gap states of a polyethylene model oligomer observed by using high-sensitivity ultraviolet photoelectron spectroscopy," *IEICE Trans. Electron.*, vol.E102-C, no.2, pp.168–171, 2019.
- [9] H.T. Baytekin, A.Z. Patashinski, M. Branicki, B. Baytekin, S. Soh, and B.A. Grzybowski, "The mosaic of surface charge in contact electrification," *Science*, vol.333, no.6040, pp.308–312, 2011.
- [10] M. Iwamoto and C.-X. Wu, *The Physical Properties of Organic Monolayers*, World Scientific, New Jersey London Singapore Beijing Shanghai Hong Kong Taipei Chennai, 2001.
- [11] X. Chen, D. Taguchi, T. Manaka, M. Iwamoto, and Z.L. Wang, "Direct probing of contact electrification by using optical second harmonic generation technique," *Sci. Rep.*, vol.5, p.13019, 2015.
- [12] D. Taguchi, T. Manaka, and M. Iwamoto, "Imaging of triboelectric charge distribution induced in polyimide film by using optical second-harmonic generation: Electronic charge distribution and dipole alignment," *Appl. Phys. Lett.*, vol.114, p.233301, 2019.
- [13] A part of this work was presented at IEICE Society Conference 2019, Osaka University, Toyonaka, Osaka, Japan, D. Taguchi, T. Manaka, and M. Iwamoto, "Visualizing polarity of electronics charges generated on rubbed PMDA-ODA polyimide surface by using electric-field-induced optical second-harmonic generation," 12 Sept. 2019, C-13-1(oral); D. Taguchi, T. Manaka, and M. Iwamoto, "EFISHG measurement system for visualizing positive and negative charges of triboelectricity generation," *IEICE Technical Report*, vol.119, no.65, OME2019-8, pp.1–7, 2019. (in Japanese)
- [14] Y.R. Shen, *The Principles of Nonlinear Optics*, John Wiley & Sons, New York, 1984.
- [15] R.W. Boyd ed., *Nonlinear Optics*, 3rd ed., Academic, London, 2008.
- [16] K. Kemnitz, K. Bhattacharyya, J.M. Hicks, G.R. Pinto, K.B. Eisenthal, and T.F. Heinz, "The phase of second-harmonic light generated at an interface and its relation to absolute molecular orientation," *Chem. Phys. Lett.*, vol.131, no.4-5, pp.285–290, 1986.

### Appendix:

Figure A·1 shows a variety of optical arrangements for SHG measurement with local oscillator trialed. Figure A·1 (a) (b) utilizes a dispersion of refractive index of air. The phase  $\theta$  between SHG from local oscillator and EFISHG is controlled by shifting location of local oscillator. Figure A·1 (c)–(f) utilizes a dispersion of refractive index of synthetic silica plate. The phase  $\theta$  between SHG from local oscillator and EFISHG is controlled by rotating the silica plate. Figure A·1 (a) was one of the best arrangements that showed clear interference of SHG from local oscillator with SHG from polyimide/Ni foil sample, and used in experimental arrangement illustrated in Fig. 2. The arrangement in Fig. A·1 (b) showed poor SHG interference probably due to a deformation of probe beam pattern after reflection at polyimide sample. The arrangements in Fig. A·1 (c)–(f) are also trialed, but are discarded for consideration of a shift of image with a rotation of silica plate.

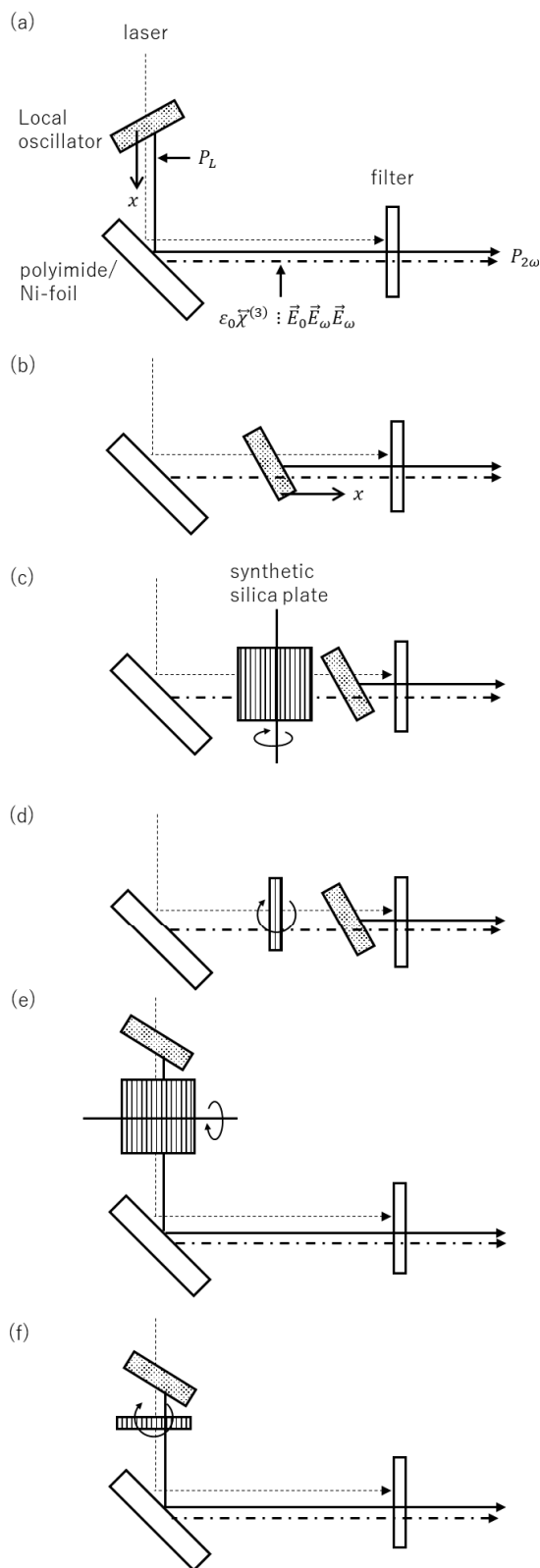


**Fig. A-1** Optical arrangement for SHG measurement with local oscillator trialed.



**Dai Taguchi** obtained M.E. and D.E. from Tokyo Institute of Technology in 2005 and 2008, respectively. He is an assistant professor of Tokyo Institute of Technology, a member of IEICE, JSAP, JLCs and the IEEEJ.



**Takaaki Manaka** graduated from Tokyo Institute of Technology and obtained B. E. in 1995. He obtained M. E. and D. E. from Tokyo Institute of Technology in 1997 and 2000, respectively. Now he is an associate professor of Tokyo Institute of Technology, a member of JSAP and the IEEEJ. His current interests focus on optical properties of organic materials, organic and molecular electronics, and liquid crystals.



**Mitsumasa Iwamoto** graduated from Tokyo Institute of Technology and obtained B. E. in 1975. He obtained M. E. and D. E. from Tokyo Institute of Technology in 1977 and 1981, respectively. He is a professor of Tokyo Institute of Technology, fellows of the JSAP, the IEICE, and the IEEEJ, etc. His current interests focus on organic electronics, mainly on the electrical, optical, physical and dielectric properties of thin films, monolayers, liquid crystals and molecules.